Magnetic anisotropy and microscopy studies in magnetostrictive Tb-(Fe,Co) thin films

K. Umadevi, , A. Talapatra, , J. Arout Chelvane, , Mithun Palit, , J. Mohanty, and , and V. Jayalakshmi

Citation: Journal of Applied Physics **122**, 065108 (2017); doi: 10.1063/1.4998451
View online: http://dx.doi.org/10.1063/1.4998451
View Table of Contents: http://aip.scitation.org/toc/jap/122/6
Published by the American Institute of Physics

Magnetic anisotropy and microscopy studies in magnetostrictive Tb-(Fe,Co) thin films

K. Umadevi,[1,2] A. Talapatra,[3] J. Arout Chelvane,[1,a)] Mithun Palit,[1] J. Mohanty,[3] and V. Jayalakshmi[2]
[1]*Defence Metallurgical Research Laboratory, Hyderabad, 500058, India*
[2]*Department of Physics, National Institute of Technology, Warangal 506004, India*
[3]*Department of Physics, Indian Institute of Technology Hyderabad, Khandi, Telangana 502285, India*

(Received 11 May 2017; accepted 31 July 2017; published online 14 August 2017)

This paper reports the effect of the film thickness on the magnetostrictive behavior of (Fe,Co) rich Tb-(Fe,Co) films grown on Si ⟨100⟩ by electron beam evaporation. Magnetostriction was found to decrease with an increase in film thicknesses. To understand the variation of magnetostriction with the film thickness, detailed structural, microstructural, magnetization, and magnetic microscopy studies were carried out. X-ray diffraction studies indicated the presence of two phases, viz., Tb_2 $(Fe, Co)_{17}$ and Fe-Co phases, for all the films. With the increase in the film thickness, the peak intensity of the Tb_2 $(Fe, Co)_{17}$ phase decreased and that of the Fe-Co phase increased. Magnetization studies showed the presence of strong in-plane anisotropy for all the films. In addition to this, the presence of the out-of-plane component of magnetization was also observed for the films grown with higher thicknesses. This anisotropic behavior was also validated through magnetic microscopy studies carried out along the in-plane and out-of-plane directions employing magneto-optic Kerr microscopy and magnetic force microscopy, respectively. The decrease in magnetostriction was explained on the basis of dual phase formation and complex interplay between the in-plane and out-of-plane magnetic anisotropies present in the film. *Published by AIP Publishing*. [http://dx.doi.org/10.1063/1.4998451]

INTRODUCTION

Amorphous Tb-Fe-Co thin films have been investigated in recent years as they exhibit strong magnetic anisotropy, high thermal stability, large magnetostriction, tunable magnetic hysteresis, and large Kerr rotation. The above mentioned properties make them suitable for several applications such as micro-actuators, micro-sensors, and magneto-optic recording media.[1–9] However, these applications strongly depend on the anisotropy present in the film, which in turn is primarily controlled by the film composition, film thickness, and microstructure.[8,10] The films exhibiting out-of-plane (OOP) magnetic anisotropy and tunable magnetic properties such as coercivity, magnetization, and squareness ratio are preferred for memory applications,[6] whereas films displaying strong in-plane (IP) anisotropy combined with large magnetostriction are best suited for micro-mechanical devices.[7,9] The magnetic phase diagram of Tb-Fe/(Fe, Co) alloy thin films shows that either films with compositions rich in the transition metal content (> 85 at. %) or films with the rare earth (Tb) content greater than 40 at. % exhibit IP magnetic anisotropy.[10,11] The magnetic phase diagram also clearly shows that films with the Tb content in the range of 40–15 at. % display strong OOP magnetic anisotropy. From the vast literature available on Tb-Fe-Co films, it is clearly evident that most of the research and development work carried out until now were predominantly focused on films with Tb compositions in the range of 40–15 at. % due to the considerable interest in increasing the storage capacity of memory devices.[3] Our recent investigation on sputter deposited Tb-Fe-Co films with the Tb content ∼50 at. % has shown weak magnetic ordering at room temperature owing to the sperimagnetic behavior arising from the amorphous nature of Tb-Fe-Co films.[12] It is therefore evident that for the development of films with high magnetostriction coupled with IP magnetic anisotropy, it is imperative to select compositions rich in the transition metal content. Further, our recent investigations on Tb-Fe thin films have shown that the film thickness was found to have a profound impact on the magnetic anisotropy.[13] In the light of the above, a detailed study was undertaken to grow Tb – 90 at. % (Fe, Co) films with different thicknesses on Si ⟨100⟩ substrates and investigate their surface morphology, structure, magnetic microstructure, and magnetostrictive properties. The manuscript significantly contributes to the spin re-orientation phenomenon in rare earth transition metal films caused by the variation in the composition (controlling magnetic anisotropy) and microstructure with the change in film thicknesses. Towards understanding the reason for the variation in magnetostriction with film thicknesses, we have explored a complete picture of magnetic domain along the IP and OOP directions, employing complementary magnetic microscopy techniques. Moreover, we have clearly indicated the transformation of magnetic domains under the rotation of the applied IP magnetic field from easy to hard magnetization direction and the mechanism of magnetization reversal therein. The variation of magnetostriction with film

a)Author to whom correspondence should be addressed: aroutchelvane@gmail.com

thickness turned out to be in good agreement with the microscopic findings.

EXPERIMENTAL DETAILS

Tb-Fe-Co films with various thicknesses, viz., 50, 200, 300, and 400 nm, were deposited on Si ⟨100⟩ substrates at room temperature by electron beam evaporation. The films were grown under vacuum (1×10^{-7} Torr) at a constant deposition rate of 5 Å/s using an alloy target with nominal composition of $Tb(Fe_{0.55}Co_{0.45})_{2.5}$. After deposition, the films were post annealed at 450 °C for 30 min under vacuum (1×10^{-7} Torr). A thin layer of chromium (~3 nm) was deposited on Tb-Fe-Co as a capping layer to avoid oxidation. Structural and microstructural studies were carried out employing an X-ray diffractometer (XRD) and a field emission gun scanning electron microscope (FEG-SEM), respectively. Compositions of the films were estimated using energy dispersive spectroscopy (EDS) attached to FEG-SEM. Room temperature magnetization measurements were carried out along the IP and OOP directions employing a vibrating sample magnetometer (VSM). The magnetostriction in thin films was calculated by measuring the tip deflection in the thin film cantilever beam with the application of an external magnetic field. A home-made tip deflection measurement set up was used for measuring the tip deflection in thin films. In this setup, the sample was held as a cantilever beam in between the poles of an electromagnet, such that the field is applied parallel to the plane of the thin film. The tip deflection on the free end of the sample was measured using a laser Doppler vibrometer.[14] IP magnetic hysteresis with simultaneous domain mapping was carried out by using a longitudinal magneto-optic Kerr effect microscope (LMOKE) at different azimuthal angles. The OOP component of magnetization was estimated from the magnetic domain images employing a magnetic force microscope (MFM).

RESULTS AND DISCUSSION

The composition of the films estimated from EDS analysis was found to be ~Tb_{10}(Fe, Co)$_{90}$ for all the films. Figure 1 shows the XRD patterns of annealed Tb-Fe-Co films deposited with various thicknesses, viz., 50, 200, 300, and 400 nm. XRD patterns clearly indicate the presence of two phases, viz., $Tb_2(Fe,Co)_{17}$ and Fe-Co.[15] With an increase in film thickness, the peak intensity of the $Tb_2(Fe,Co)_{17}$ phase decreases and that of the Fe-Co phase increases. The phase formation at the selected composition, viz., Tb_{10}(Fe, Co)$_{90}$, is in agreement with the binary Tb-Fe and Tb-Co phase diagrams, which indicates the formation of a phase mixture consisting of Fe-Co and $Tb_2(Fe,Co)_{17}$. The $Tb_2(Fe,Co)_{17}$ phase is formed by a peritectic reaction, viz., L (Liquid) +Fe-Co → $Tb_2(Fe,Co)_{17}$. For the films grown with lower thicknesses, the peritectic reaction is largely suppressed owing to the high cooling rate achieved during the deposition process. However, for the films deposited with a higher thickness, the peritectic reaction could not be suppressed completely, due to the lower cooling rate achieved, and as a result, more volume fraction of the unreacted properitectic Fe-Co phase has been observed. The decrease in the cooling rate with the increase in the film thickness can be correlated with the low heat transfer owing to growth of several layers and the possibility of localized heating of the substrate because of its interaction with the evaporated adatoms. Figures 2 and 3 show the surface and cross-sectional microstructures of Tb-Fe-Co films grown with different thicknesses. For the 50 nm thick film, a fine island kind of morphology has been observed. However, with the increase in the film thickness, the surface microstructure indicated the presence of triangular shaped grains whose sizes increased with the increase in film thicknesses (Fig. 3). This could be probably due to the minimization of surface energy of the films. The cross sectional microstructure also indicated fine features for the 50 nm thick film, whereas columnar growth of fine grains has been noticed for the films grown with higher thicknesses (Fig. 3). The column height was found to extend up to the surface of the film with a triangular shape at the top end.

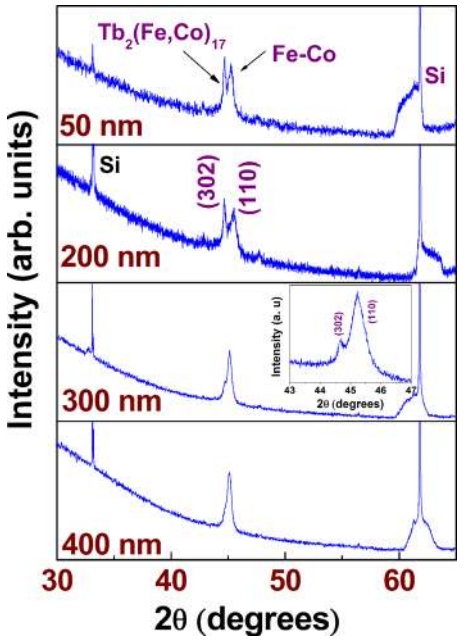

FIG. 1. XRD patterns of Tb-Fe-Co films grown with different thicknesses. The inset shows the presence of both $Tb_2(Fe,Co)_{17}$ and Fe-Co phases.

Figure 4 shows IP and OOP room temperature magnetization curves of Tb-Fe-Co films grown with different thicknesses. Magnetization curves showed the presence of strong IP anisotropy for all the films with low coercivity. The formation of strong IP anisotropy can be attributed to the high transition metal content present in the films. The saturation magnetization calculated along the IP and OOP directions was found to be high when compared with the magnetization values reported in the literature owing to the high (Fe,Co) content in the film.[3,16] The magnetization values estimated from the magnetization curves are shown in Table I. The formation of the nano-crystalline Fe-Co phase favoring IP magnetic anisotropy in Tb-Fe-Co thin films has been reported by Umadevi *et al.*[8] In addition to the strong IP magnetic anisotropy, the presence of OOP magnetic components was also observed from the OOP magnetization curves. It is also evident that OOP coercivity increases with the increase in film

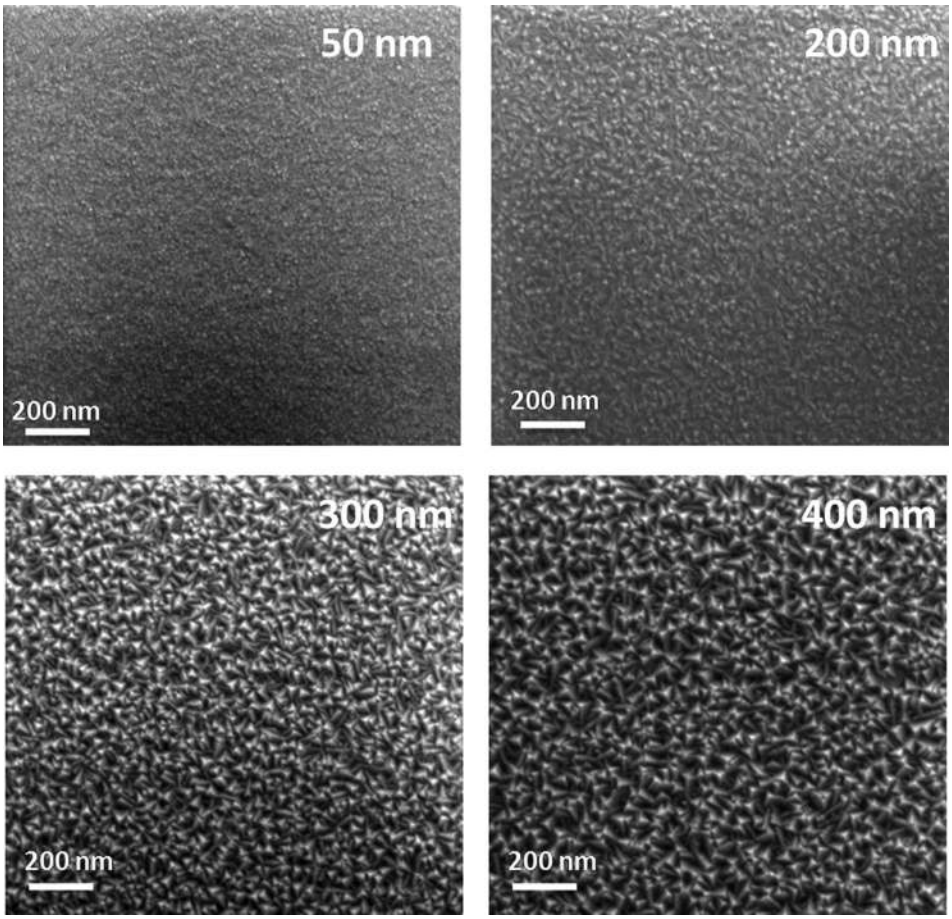

FIG. 2. Surface morphology of Tb-Fe-Co films grown with different thicknesses.

thicknesses. The possible reason for the formation of OOP magnetic components with the increase in the film thickness can be correlated with the columnar growth of fine grains as observed from the cross-sectional microstructural investigations [Fig. 2(b)]. The presence of the columnar morphology giving rise to strong perpendicular magnetic anisotropy has been reported recently in Tb-Fe-Co thin films.[8] The co-existence of IP and OOP components clearly indicates the presence of mixed anisotropies around this composition range [viz., $Tb_{10}(Fe, Co)_{90}$] although it is predominantly reported that films rich in the transition metal content exhibit only IP magnetic anisotropy.[10,11]

The variation in IP room temperature magnetostriction with the film thickness shows that the magnetostriction values decrease with the increase in film thicknesses (Fig. 5). The decrease in magnetostriction with increasing film thicknesses can be attributed to the change in the phase volume fraction of different phases as observed from the XRD studies. It can be observed that the films with lower thicknesses contain a high volume fraction of the $Tb_2(Fe,Co)_{17}$ phase, which is known for large magnetostriction owing to their high magneto-crystalline anisotropy. On the other hand, the films with higher thicknesses largely consist of Fe-Co solid solution, which exhibits a much lower value of magnetostriction.

In addition to this, the decrease in magnetostriction with the increase in the film thickness can also be correlated with the presence of OOP magnetic components exhibited by the films. With the magnetic field applied along the IP direction, the presence of OOP magnetic components offsets the magneto-elastic coupling along the IP direction, which in turn reduces the overall bending of the film-substrate assembly. To unravel the observed magnetostrictive behaviour further, magnetic microscopy studies were carried out along the IP and OOP directions employing longitudinal MOKE and MFM, respectively.

The hysteresis loops with simultaneous domain imaging along the IP direction was measured employing a MOKE microscope in the longitudinal mode. The background subtraction method was carried out to enhance the signal from the sample. Hysteresis loops were traced by evaluating the contrast difference between the two oppositely magnetized domain patterns with respect to the variation in magnetic fields. To investigate the nature of IP magnetic anisotropy, the position of the sample was fixed and the magnetic field was swept at different azimuthal angles ($\Theta = 0$–$360°$) with respect to the plane of the film at an increment of 5°. From the angular dependent hysteresis measurements, the direction along which the film exhibits maximum coercivity was identified as the easy direction of magnetization. Taking this point as reference, the magnetic field angle was varied with respect to the plane of the film. Figures 6(A), 6(B), and 6(C) show the static hysteresis loops and domain images along the easy and hard axes of magnetization for the films deposited with different thicknesses, viz., 50, 200, and 300 nm, respectively. When the magnetic field was applied along the easy direction of magnetization, domains are found to be nucleated at the sample edge. With a subsequent increase in the magnetic field, the nuclei propagate along the magnetic field direction and wider

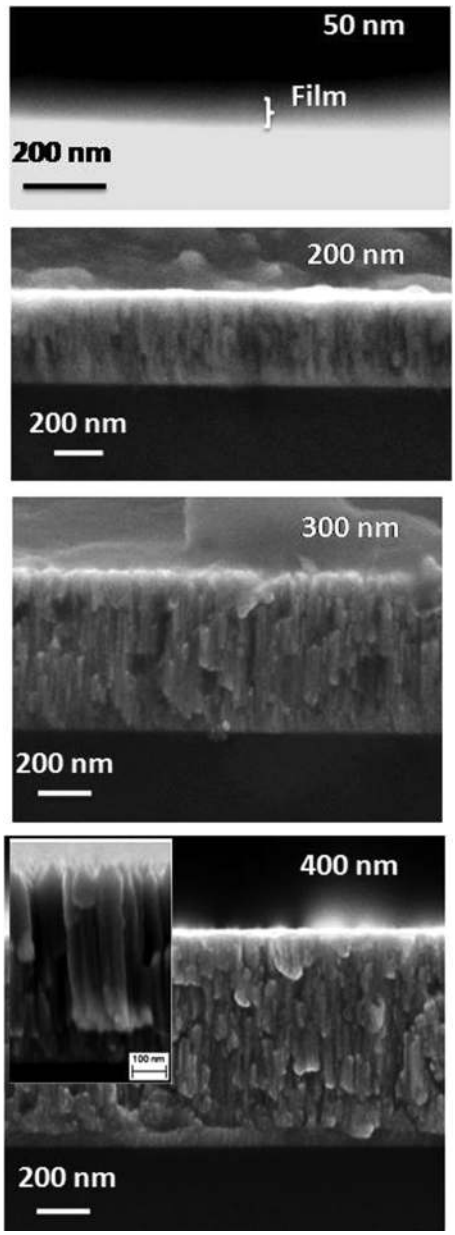

FIG. 3. Cross-sectional microstructures of Tb-Fe-Co films grown with different thicknesses. The inset shows the columnar growth with the conical end at the top.

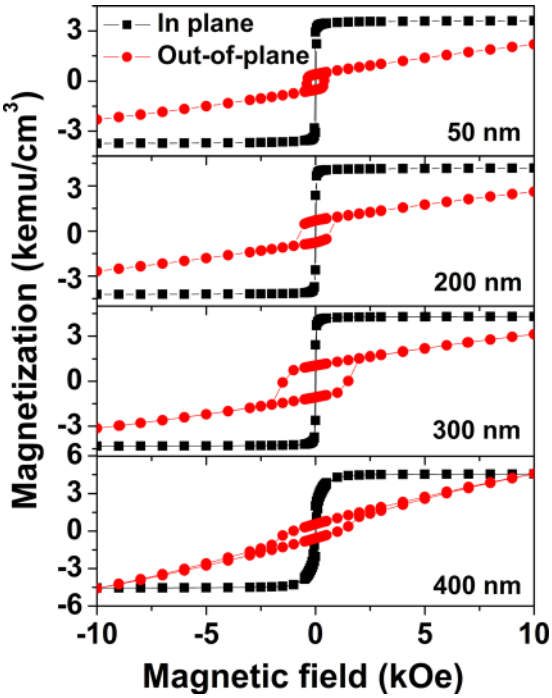

FIG. 4. IP and OOP magnetization curves of Tb-Fe-Co films grown with various thicknesses.

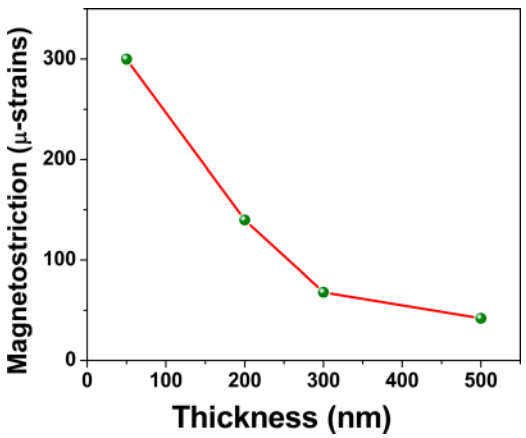

FIG. 5. Variation of saturation magnetostriction with film thickness for Tb-Fe-Co films.

band domains were formed which are separated by conventional 180° domain walls. These domains further rearrange themselves due to the change in the distribution of the demagnetizing fields. It is also observed that the periodicities of the domains change when the magnetic field is applied away from the easy direction of magnetization. On top of that, a ripple-like domain pattern was observed, when the magnetic field was applied along the hard direction of magnetization, which is the usual signature for hard axis behavior in polycrystalline films.[17–20] The suppression of stray field energy due to the characteristic magnetic fluctuation connected with the polycrystalline microstructure is the reason for the creation of

TABLE I. Film thickness, IP & OOP magnetization and summary of main results extracted from MFM images presented in Fig. 8.

Film thickness (nm)	IP saturation magnetization (emu/cm^3)	OOP magnetization at 10 kOe (emu/cm^3)	Magnetic phase contrast (deg)	Area between two sharp peak (from histogram analysis)
50	3600	2300	0.5	Two sharp peaks are absent
200	4100	2700	2.6	80%
300	4300	3000	2.9	74.5%
400	4600	4500	2.6	76.6%

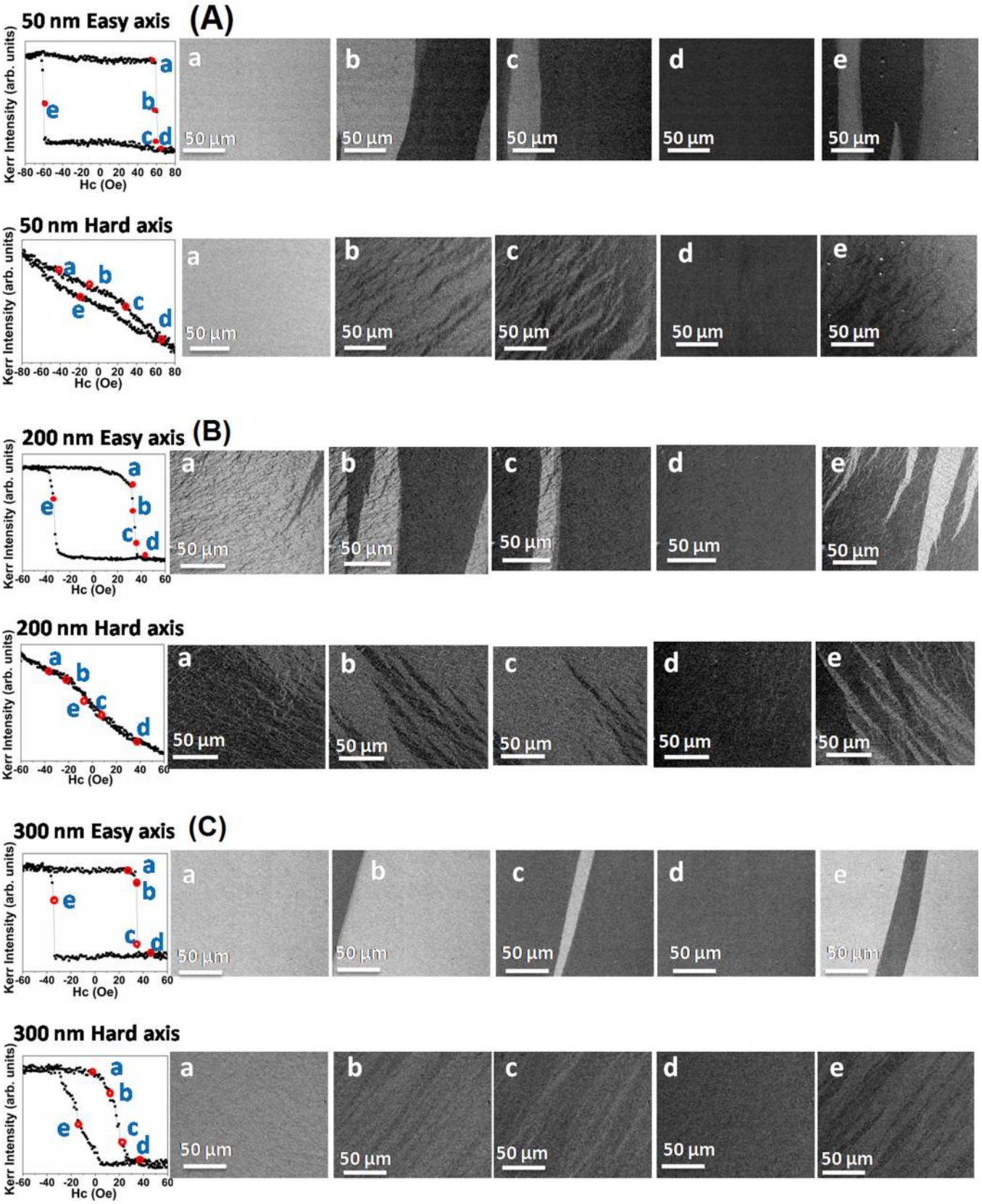

FIG. 6. LMOKE microscopy carried out along the easy and hard axes of magnetization for Tb-Fe-Co films grown with (A) 50 nm, (B) 200 nm, and (C) 300 nm.

ripple domains stabilizing 90° domain walls.[17] Further, it is also worth noting that the orientation and the period of the domains are strongly dependent on the material characteristics such as thickness, stress, and surface morphology. The domain periodicity seems to be more for the case of the 300 nm film, where the number of oppositely magnetized domains is less within the same field of view at similar field values as shown in Fig. 6(C).

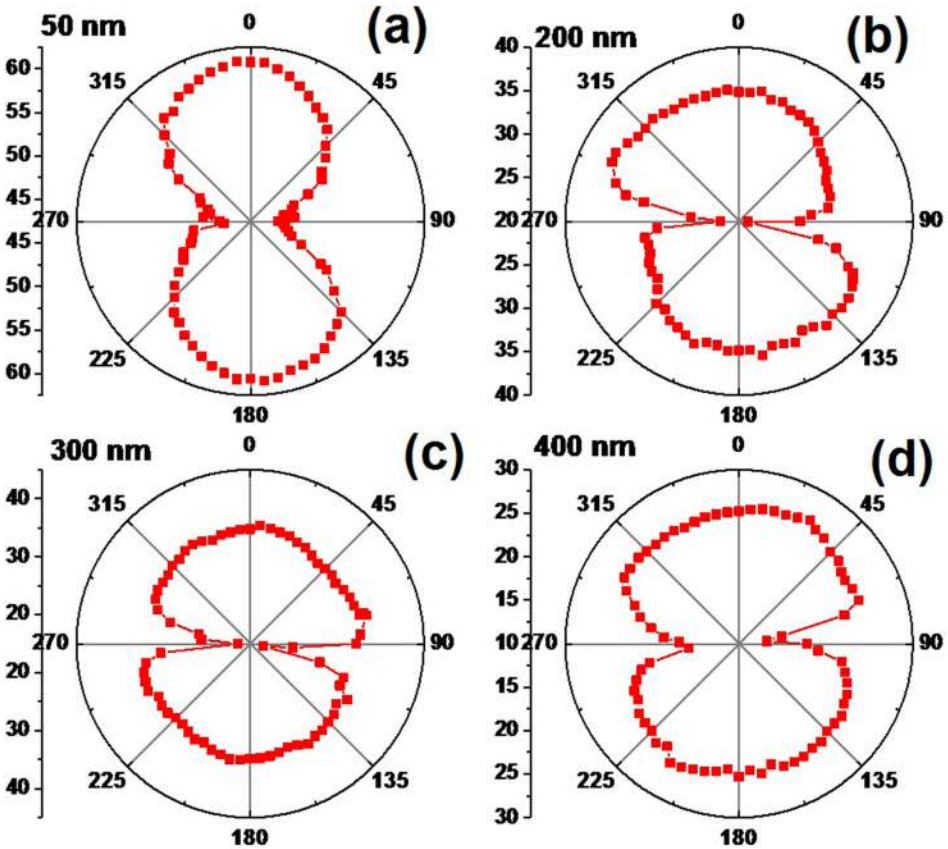

FIG. 7. Polar plot displaying the variation of coercivity with different azimuthal angles for Tb-Fe-Co films grown with different thicknesses.

The hysteresis loop measured along the easy direction of magnetization for the 50 nm thick film [Fig. 6(A)] shows a square loop with the domains nucleating around the coercive field where sharp reversal in magnetization occurs ($H_c = 60$ Oe). Along the hard direction, the magnetization is changed in a continuous way with the domains nucleating at a coercive field of 48 Oe. However, the shape of the loop deviates from a square like loop observed earlier. With a further increase in the magnetic field, the magnetization reaches positive saturation around 60 Oe along the hard axis. Along the easy direction of magnetization, since the nucleation field is comparable with the coercive field, it is expected that the magnetization reversal is dominated by rapid domain wall motion. A similar trend in the hysteresis has been observed for the films grown with higher thicknesses (Fig. 6). However, along the hard axis of magnetization, the magnetization reversal is found to be predominantly dominated by domain wall rotation.

To study the IP magnetic anisotropy further, coercivity variation as a function of various azimuthal angles Θ has been carried out and is illustrated in Figs. 7(a), 7(b), 7(c), and 7(d) for Tb-Fe-Co films with thicknesses of 50, 200, 300, and 400 nm, respectively. The presence of symmetric two-fold lobes in the polar plot essentially signifies the presence of uni-axial anisotropy for all the films.[21] Further, it is also observed that the magnitude of coercivity along the IP direction is found to be maximum for the 50 nm thick film, and with a subsequent increase in film thickness, the coercivity decreases. This indicates that the IP magnetic anisotropy shows a decreasing trend with increasing film thickness. The magnetization measurements also indicate an increase in OOP coercivity which further hints about the development of OOP magnetic anisotropy for the films grown with higher thicknesses.

Complementary microscopy studies have been performed with magnetic force microscopy where the magnetized tip is more sensitive to the OOP component of the stray field emanating from the film surface. The lift height of the magnetized tip was set at 50 nm to minimize the short-range topographic contribution. Figure 8 shows the MFM images for the Tb-Fe-Co films grown with different thicknesses, viz., 50, 200, 300, and 400 nm. The MFM contrast for the 50 nm thick film was found to be very weak, indicating the absence of the appreciable OOP component. However, with the increase in film thickness, MFM images indicated the presence of significantly strong magnetic contrast. It is also observed that the domains are aperiodic and patch type for the films grown with higher thicknesses. Assuming the magnetization of the tip to be identical for all the measurements, the magnetic phase difference can be taken as a figure of merit to evaluate the strength of the magnetic signal. With an increase in film thickness, the magnetic phase contrast from the oppositely magnetized domains is found to increase (Table I). Although magnetic phase contrast gives a qualitative idea about the increase in the OOP components, quantitative evaluation of OOP magnetic components with thickness variation is difficult owing to the aperiodic nature of magnetic domains. Therefore, efforts were made to quantify the MFM images through histogram analysis which essentially describes the area under different magnetic contrasts.[22] Ideally, for materials with strong OOP magnetic anisotropy, the histogram should display two sharp distinct

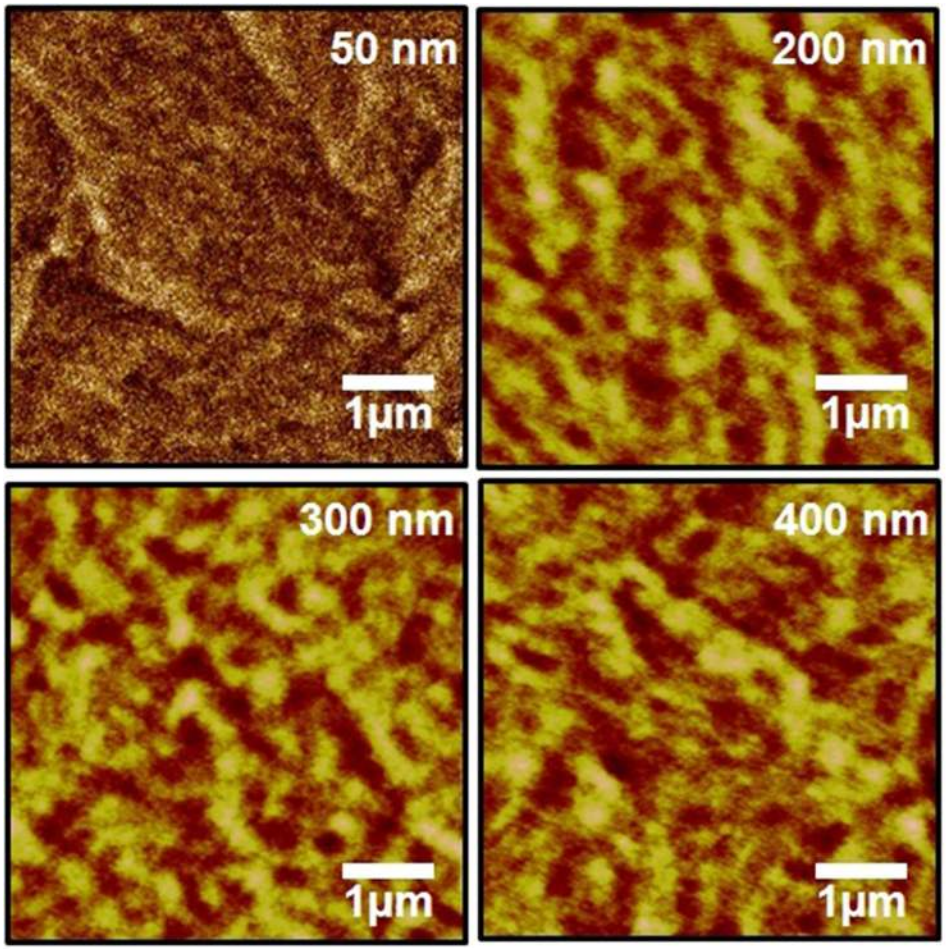

FIG. 8. MFM images of Tb-Fe-Co films grown with different thicknesses.

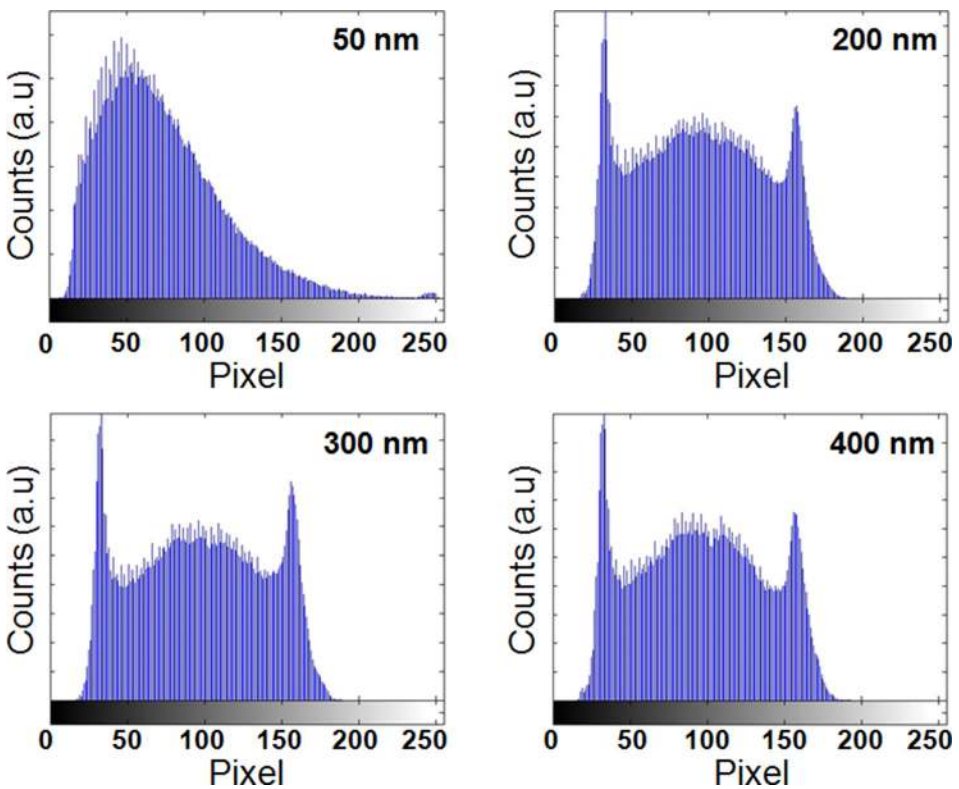

FIG. 9. Histograms analysis indicating the area under different magnetic contrasts from MFM images.

peaks (corresponding to the oppositely oriented domains) having a continuous transition between them. The area intermediate between the two sharp peaks can quantify the improvement or deterioration of OOP components in the sample. Assuming the total area to be 100%, the intermediate area, viz., the area between the sharp peaks can be estimated by subtracting the area under the two sharp peaks from the total area. Figure 9 shows the calculated magnetic contrast histograms for the films grown with different thicknesses. The 50 nm thick film does not indicate any sharp distinct peak. The broad distribution of contrast variation for the 50 nm thick Tb-Fe-Co film indicates the absence of oppositely magnetized domains along the OOP direction. Nevertheless, two distinct peaks with broad and continuous transition have been observed for the thicker films. The estimated intermediate area for the films deposited with different thicknesses is displayed in Table I. From Table I, it is clearly evident that with the increase in film thickness, the numerical value determined from the histogram decreases, indicating an increase in OOP components. The OOP component of magnetization grows on top of IP magnetic anisotropy with increasing thickness and attains the maximum value for the 400 nm thick film.

From the detailed surface and magnetic microscopy studies, it is clear that the 50 nm thick film exhibits large magnetostriction due to the presence of strong IP magnetic anisotropy. However, with the increase in film thickness, the presence of OOP magnetic components co-existing with IP magnetic anisotropy offsets the overall magnetostriction values. This study clearly shows the complex interplay between the IP and OOP components in modifying the magnetic behavior of transition metal rich Tb-Fe-Co films.

CONCLUSIONS

Fe-Co rich Tb-(Fe-Co) films with various thicknesses were deposited on Si ⟨100⟩ substrates employing the electron beam evaporation technique at room temperature. The structural and magnetic properties evaluated from these films are summarized below:

(1) Structural analysis revealed the presence of two phases, viz., $Tb_2(Fe,Co)_{17}$ and Fe-Co, for all the films. With the increase in film thickness, the volume fraction of the $Tb_2(Fe,Co)_{17}$ phase is found to decrease.
(2) Surface and cross-sectional microstructures displayed the presence of triangular shaped grains and columnar morphology, respectively, for the films grown with higher thicknesses.
(3) Magnetization studies showed the presence of strong IP anisotropy co-existing with some OOP components.
(4) Magnetostriction was found to reduce with the increase in film thickness owing to the increase in OOP components and evolution of dual phases in different volume fractions.
(5) IP uni-axial anisotropy has been observed for all the films. Magnetization reversal occurs through domain wall motion and domain wall rotation along easy and hard axes of magnetization, respectively.

ACKNOWLEDGMENTS

The authors thank Director, DMRL for the support and encouragement. The authors also thank Professor A. Arockiarajan, Department of Applied Mechanics, IIT Madras, India, for the magnetostriction measurements.

[1]M. Mansuripur, *Physical Principles of Magneto-Optical Recording* (Cambridge University Press, Cambridge, 1995).
[2]S. Tsunashima, J. Phys. D: Appl. Phys. **34**(17), R87 (2001).
[3]N. Anuniwat, M. Ding, S. J. Poon, S. A. Wolf, and J. Lu, J. Appl. Phys. **113**, 043905 (2013).
[4]M. Nakayama, T. Kai, N. Shimomura, M. Amano, E. Kitagawa, T. Nagase, M. Yoshikawa, T. Kishi, S. Ikegawa, and H. Yoda, J. Appl. Phys. **103**, 07A710 (2008).
[5]C. Lee, L. Ye, T. Hsieh, C. Huang, and T. Wu, J. Appl. Phys. **107**, 09C712 (2010).
[6]H. Ohmori, T. Hatori, and S. Nakagawa, J. Appl. Phys. **103**, 07A911 (2008).
[7]T. Honda, K. I. Arai, and M. Yamaguchi, J. Appl. Phys. **76**, 6994 (1994).
[8]K. Umadevi, S. Bysakh, J. A. Chelvane, S. V. Kamat, and V. Jayalakshmi, J. Alloys Compd. **663**, 430 (2016).
[9]Y. Torii, H. Wakiwaka, T. Kiyomiya, Y. Matsuo, Y. Yamada, and M. Makimura, J. Magn. Magn. Mater. **290-291**, 861 (2005).
[10]N. Anuniwat, Ph.D. thesis, University of Virginia, 2015.
[11]Y. Mimura, N. Imamura, and T. Kobayashi, IEEE Trans. Magn. **12**, 779 (1976).
[12]K. Umadevi, J. Arout Chelvane, H. Basumatary, M. Ramudu, S. V. Kamat, and V. Jayalakshmi, J. Magn. Magn. Mater. **418**, 163 (2016).
[13]K. Sai Maneesh, J. Arout Chelvane, A. Talapatra, H. Basumatary, J. Mohanty, and S. V. Kamat, "Spin reorientations in Tb-Fe films grown on polyimide substrates," J. Magn. Magn. Mater. (published online).
[14]H. Mishra, J. Arout Chelvane, and A. Arockiarajan, Sens. Actuators A **235**, 218 (2015).
[15]S. Charfeddie, K. Zehani, L. Bessais, and A. Korchef, J. Solid State Commun. **238**, 15 (2016).
[16]A. Chekanov, K. Matsumoto, and K. Ozaki, J. Appl. Phys. **90**, 4657 (2001).
[17]A. Hubert and R. Schäfer, *Magnetic Domains* (Springer, New York, 1998).
[18]O. Idigoras, A. K. Suszka, P. Vavassori, P. Landeros, J. M. Porro, and A. Berger, Phy. Rev. B **84**, 132403 (2011).
[19]N. Chowdhury and S. Bedanta, AIP Adv. **4**, 027104 (2014).
[20]S. Mallik, S. Mallick, and S. Bedanta, J. Magn. Magn. Mater. **428**, 50 (2017).
[21]Q. Wu, W. He, H.-L. Liu, J. Ye, X.-Q. Zhang, H.-T. Yang, Z.-Y. Chen, and Z.-H. Cheng, Sci. Rep. **3**, 1547 (2013).
[22]P. Saravanan, A. Talapatra, J. Mohanty, J.-H. Hsu, and S. V. Kamat, J. Magn. Magn. Mater. **432**, 82 (2017).